SUB-10^{-16} FREQUENCY STABILITY IN THE JPL MULTI-POLE LINEAR ION TRAP STANDARD

E. A. Burt, D. G. Enzer, R. T. Wang, W. A. Diener, and R. L. Tjoelker
Jet Propulsion Laboratory, California Institute of Technology
Pasadena, CA 91109-8099, USA
E-mail: *eric.a.burt@jpl.nasa.gov*

Abstract

The JPL Multi-pole Linear Ion Trap Standard (LITS) has demonstrated excellent short- and long-term frequency stability and reduced sensitivity to its three primary systematic effects: the second-order Doppler shift and second-order Zeeman shift and the pressure shift. In this paper, we report developments that reduce the sensitivity to all residual systematic effects to less than 5×10^{-17} and show initial long-term comparisons with other highly stable clocks. Using GPS Carrier Phase Time Transfer over a 2-month period the LITS deviated from UTC (USNO) by no more than ± 1 ns in phase and had a frequency drift of $0.2(3.0) \times 10^{-17}$/day. We also report a new mode of operation that enables further improved short-term stability to less than $5 \times 10^{-14}/\tau^{1/2}$, and an atomic line Q of 5×10^{12}, the highest ever demonstrated in a microwave atomic standard operating at room temperature. With these advances, the multi-pole LITS provides a new and unique timekeeping and reference capability in the JPL Frequency Standards Test Laboratory, with broader applicability to national metrology and timekeeping laboratories.

INTRODUCTION

Continuously running frequency standards with state-of-the-art frequency stability are required for timekeeping and deep space tracking applications. Doppler spacecraft tracking, VLBI, and radio science activities require high frequency and time stability to accurately locate and direct space craft, precisely time send and receive signals, or to correlate signals received in different locations. Linear Ion Trap Standards (LITS) developed at the Jet Propulsion Laboratory (JPL) have demonstrated excellent short [1,2] and long-term stability [3] and have also demonstrated long-term field operation. The relative insensitivity to the second-order Doppler shift using a multi-pole linear ion trap configuration [4] has resulted in a Hg^{+} frequency standard with excellent long-term stability [5]. It has been shown that sensitivity to the second-order Doppler shift can be further reduced by introducing a small magnetic inhomogeneity [18]. In this paper, we describe this technique, as well as other methods used to further reduce the primary multi-pole LITS systematic sensitivities. We will then show the results of the first long-term comparisons made between this LITS and other high-performance clocks. This advanced multi-pole LITS standard provides a new capability for timekeeping and serves as an unambiguous performance reference of other very stable atomic standards and global time and frequency transfer methods.

THE MULTI-POLE LITS: CONFIGURATION AND PAST PERFORMANCE

The multi-pole LITS evolved from its predecessor, the quadrupole LITS, in an effort to improve LITS long-term stability. The motivation for developing long-term ultra-stable continuously running frequency standards at the Jet Propulsion Laboratory (JPL) is three-fold: 1) long-term characterization of time transfer methods that is not limited by clock performance, 2) characterization of JPL Deep Space Network masers, and 3) for possible use in metrology labs as a replacement for time-keeping "fly wheels" consisting of atomic clock ensembles.

The configuration of the advanced multi-pole LITS has been described elsewhere [18]. It consists of a conventional quadrupole trap (where ion loading, state selection, and state detection take place) and a multi-pole trap (where the sensitive microwave interrogation takes place). After loading and state selection, ions are "shuttled" into the multi-pole trap by varying the relative trap DC biases. After microwave interrogation, ions are shuttled back to the quadrupole trap for state detection. This configuration not only takes advantage of the reduced second-order Doppler shift in the multi-pole trap, but also separates microwave interrogation from the various perturbations associated with the loading region. Component choices were dictated by the requirement for long-term operation and simplicity. No lasers, cryogenics, or microwave cavities are employed in the design.

The systematic sensitivities of the multi-pole LITS are summarized in [18]. The largest of these are ion-number-dependent effects, the second-order Zeeman shift, and the pressure shift due to collisions between trapped mercury ions and the background buffer gas. The source of each of these – the number of ions trapped, the average magnetic field in the interrogation region, and the background pressure – remain uncontrolled for simplicity and operational robustness, yet a version of the multi-pole LITS delivered to the US Naval Observatory (USNO) known as LITS-8 has already demonstrated outstanding long-term performance with a drift of less than 2×10^{-16}/day relative to UTC (USNO) [5]. LITS-8 has also run continuously for periods of up to 1 year without intervention. The multi-pole LITS has demonstrated an excellent short-term performance of $7\times10^{-14}/\tau^{1/2}$ [16] (the older quadrupole LITS demonstrated a short-term performance of $2\times10^{-14}/\tau^{1/2}$ [1,2], but didn't have the long-term stability of the multi-pole LITS).

Two versions of the multi-pole LITS have been developed. In addition to LITS-8 operating at USNO, another version known as LITS-9 exists at JPL and is the subject of this paper. A smaller, third multi-pole standard is being developed for possible space flight applications [9-11]. A very small physics unit has recently been constructed using a sealed vacuum system, showing excellent signal-to-noise and short-term performance [12].

ION-NUMBER-DEPENDENT EFFECTS

Previously, the LITS second-order Doppler shift effect has been characterized by varying the trapped number of ions. However, there are three ways that varying the ion number can affect the LITS clock frequency. Two of these are due to the second-order Doppler shift in an ion trap: one due to the temperature of the ions, which is indirectly related to the ion number, and the

other due to geometric effects that are exacerbated by trapped ion number changes. For the second component, as ion number is increased, space charge repulsion causes the ion cloud volume to increase, thereby increasing the average rf trap amplitude experienced by the ions. The amplitude of the ion micro-motion is proportional to the rf trap potential, hence a number-dependent second-order Doppler shift. Since this effect scales with $-\langle v^2/c^2 \rangle$, a second-order Doppler shift has a negative slope when plotted against an increasing ion number. This effect is greatly reduced in a multi-pole trap, because the trap potential approximates a square well and the average rf amplitude experienced by the ions is much smaller than in a quadrupole trap. A third ion number effect is magnetic in origin. Care is taken in the multi-pole LITS to create a uniform magnetic field in the interrogation region by using an extended "C-field" solenoid. However, due to the finite solenoid length some fringing in the field exists at the ends, which overlap the trap volume. As the ion number is increased, the ion cloud volume increases and experiences a different value of $\langle B^2 \rangle$, where the average is taken over the ion cloud volume, as shown schematically in Fig. 1.
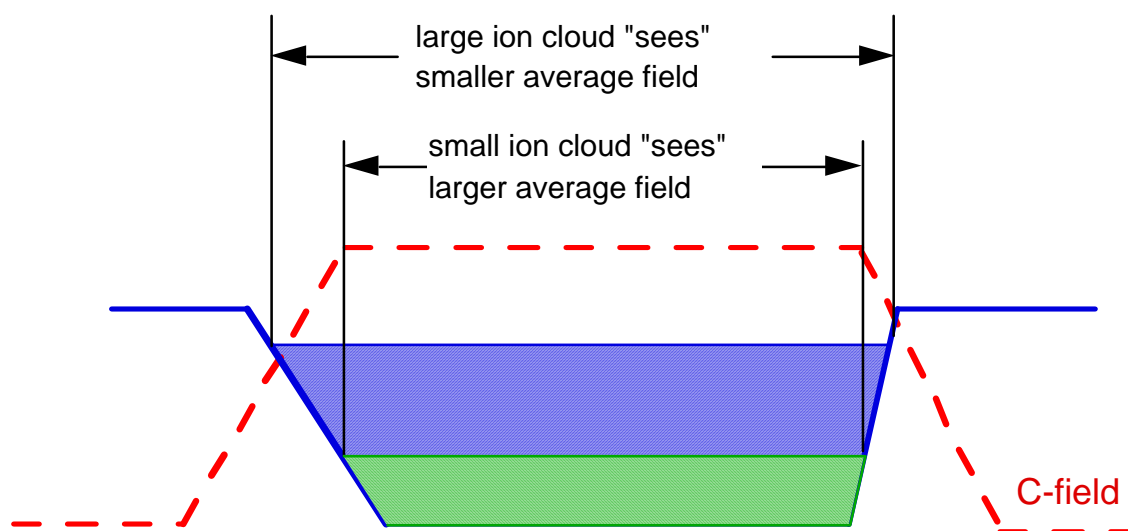

Figure 1. A schematic representation of the trap potential cross section (blue solid line) in the axial direction superimposed with a C-field (red dashed line) that has fringing at the ends. In this example, as the ion cloud volume increases, the value of $\langle B^2 \rangle$ decreases and so does the magnetic component of the ion-number-dependent shift. The effect is conceptually similar, though smaller, in the radial direction.

Due to fringing, $\langle B^2 \rangle$ decreases with ion cloud volume and, therefore, with increasing ion number as well, leading to a decreasing second-order Zeeman shift. In this case, the slope of the shift, when plotted against ion number, is negative, as with the number-dependent second-order Doppler shift. However, the ends of the solenoid are also very close to the endcaps of the inner two magnetic shield layers, which can cause a slight field increase in that region. If the field increases near the solenoid ends, then the slope of the magnetic inhomogeneity effect will be positive. Thus, the combination of the number-dependent second-order Doppler shift and the number-dependent second-order Zeeman shift can lead to either a positive or negative slope for the frequency shift as a function of ion number. The number-dependent effect in the multi-pole

LITS has been previously correlated with changes in the average magnetic field using the field-sensitive m=0 to m= ±1 transitions **[7]**.

ION-NUMBER DEPENDENCE IN LITS-8

To change the number of ions trapped and characterize number-dependent effects, we generally change the endcap DC bias voltage for the load trap. Another approach is to vary the mercury oven temperature. Each of these approaches results in ion number changes, but has different sensitivities to other systematic effects, so a consistent result using both methods gives a higher degree of confidence. Previous characterizations of ion-number-dependent effects in the LITS used the DC bias voltage method **[7]**. Recently, however, the LITS-8 mercury source was replenished at the USNO. The mercury oven temperature was subsequently increased in several steps over a 6-month period. During this time, the LITS-8 frequency offset was monitored, allowing the characterization of ion-number-dependence using the oven temperature method. Fig. 2 shows the clock resonance signal size and frequency offset during this period of mercury oven temperature changes plotted on the same graph.
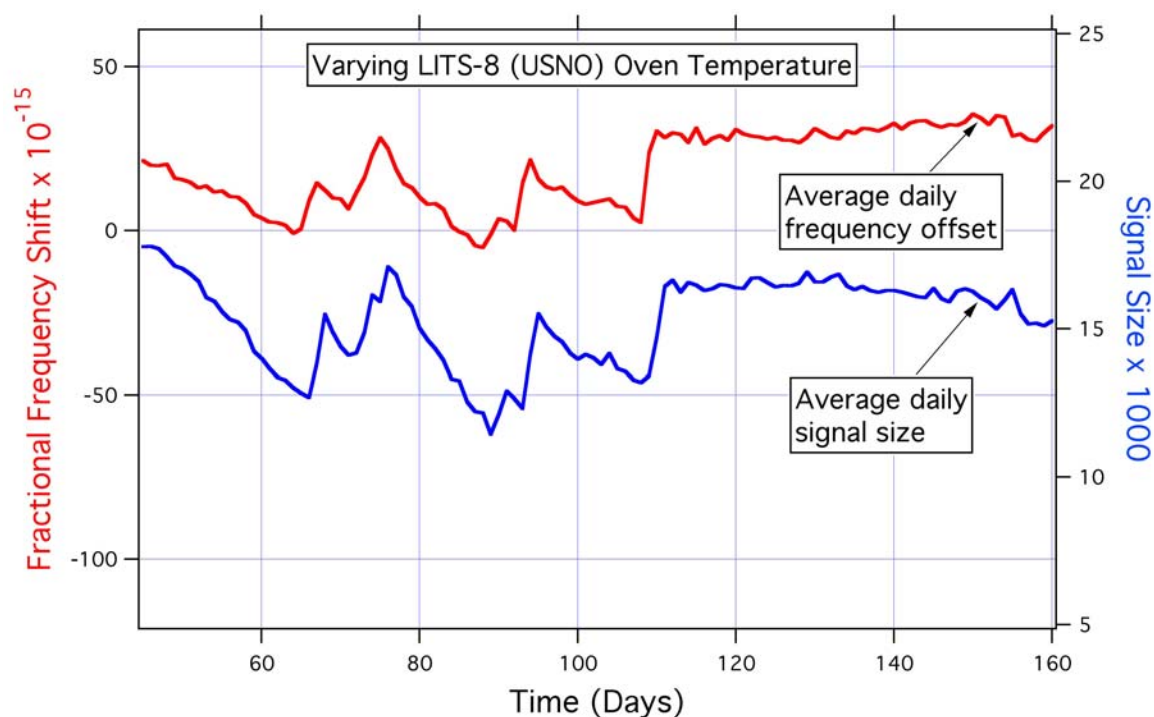

Figure 2. Fractional frequency shift and signal size data for LITS-8 over a 6-month period from November 2004 to May 2005. In these data, only the oven temperature is changed to achieve different trapped ion numbers. Frequency offsets are measured from an H-maser referenced to the USNO Master Clock. Signal size is assumed to be proportional to trapped ion number. Jumps in the signal size were due to discrete changes in the mercury oven temperature.

In these data, variations in trapped ion number of 30% achieved by varying the mercury oven temperature corresponded to a frequency shift of 1 mHz or a fractional frequency shift of about

2.5x10^{-14}. This is in very good agreement with the previous result found by varying the load trap DC bias **[7]**. The correlation between the frequency offset and changes in signal size (due to discrete changes in the mercury oven temperature that are not part of normal clock operation), which is assumed proportional to ion number, is evident. This implies that most of the frequency deviation from the USNO Master Clock observed previously **[5]** is due to this effect. In as far as we are able to mitigate ion-number dependence, we are likely to improve stability by equal measure.

MODELING ION NUMBER DEPENDENCE

Having verified that the long-term frequency stability is affected by changes in ion number and suspecting that the sensitivity has a magnetic component, we turn to modeling the effect of magnetic field inhomogeniety in the multi-pole region of the physics package. The trap, solenoid, and shields have azimuthal symmetry, allowing use of a 2-D finite element model to determine the field everywhere in the volume contained by the quadrupole and multi-pole traps. The model includes the magnetic shields, the C-field solenoid, and a number of auxiliary coils that will be described below. These represent the components that determine the magnetic environment of the physics package except external perturbations, which are small on the scale of interest.

Due to physical constraints at the interface between the quadrupole and multi-pole traps, the end of the C-field solenoid in this region is close to the end of the multi-pole trap. Since field inhomogeneity is expected to be largest here, we add into the model an auxiliary coil, "AUX1," at this end of the multi-pole trap interrogation region to modify the field at this location. Fig. 3 shows the magnitude of the modeled field along the axis of the physics package. The indicated multi-pole trap region is where microwave interrogation takes place. This figure shows how the field is quite uniform at the lower end (z = 0), but not as uniform at the upper end. While improved uniformity will be designed in the next version of this clock, the addition of a trim coil can significantly reduce nonuniformities. The dashed line shows improved uniformity with the application of a current in AUX1.

The average frequency shift for the second-order Zeeman shift in Hg$^+$ is:

$$\langle \Delta f \rangle = 9.7 \times 10^9 \frac{Hz}{T^2} \langle B_0^2 \rangle, \tag{1}$$

where the average of the field squared is taken over the volume of the trap occupied by the ions. As the ion number is changed, space charge repulsion will cause the ion cloud to change its occupation volume in the trap. Fig. 4 shows how the model predicts this average frequency shift varies with radial occupation while holding axial occupation fixed at a value of 95%. Each curve in Fig. 4 can be viewed as qualitatively showing how frequency will vary with ion number for a particular setting of the AUX1 coil.
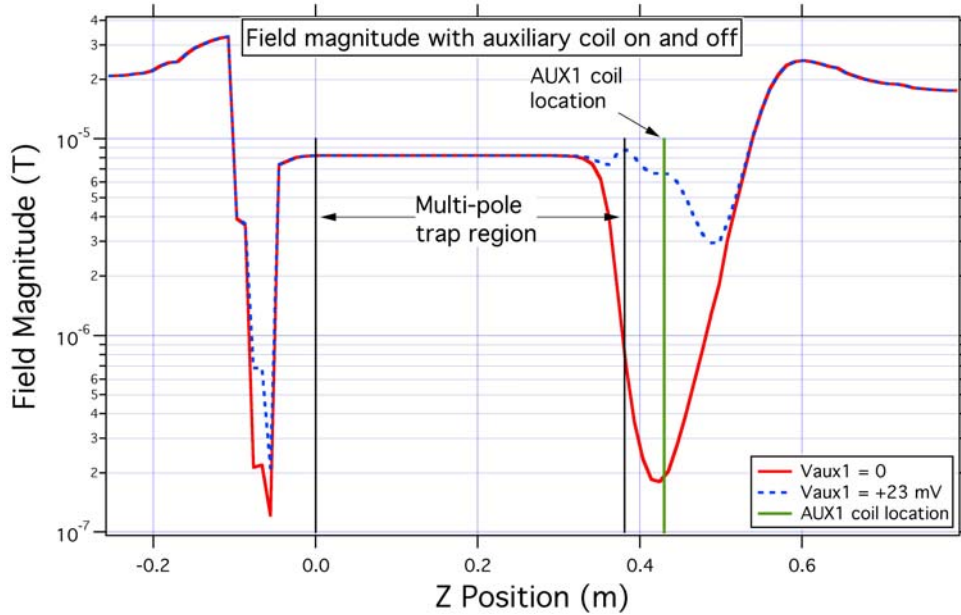
Figure 3. A plot of the modeled magnetic field magnitude along the axis of the LITS-9 physics package. The solid red line shows the field with only the C-field on. The dashed blue line shows that field modified by the application of the auxiliary coil at the interface between the quadrupole and multi-pole traps (the green line shows the location of the AUX1 coil at z ~ 0.43m), which is also at one end of the C-field solenoid. The axial position of 0 m corresponds to the lower end of the C-field and the region between the vertical black lines corresponds to the multi-pole trap.
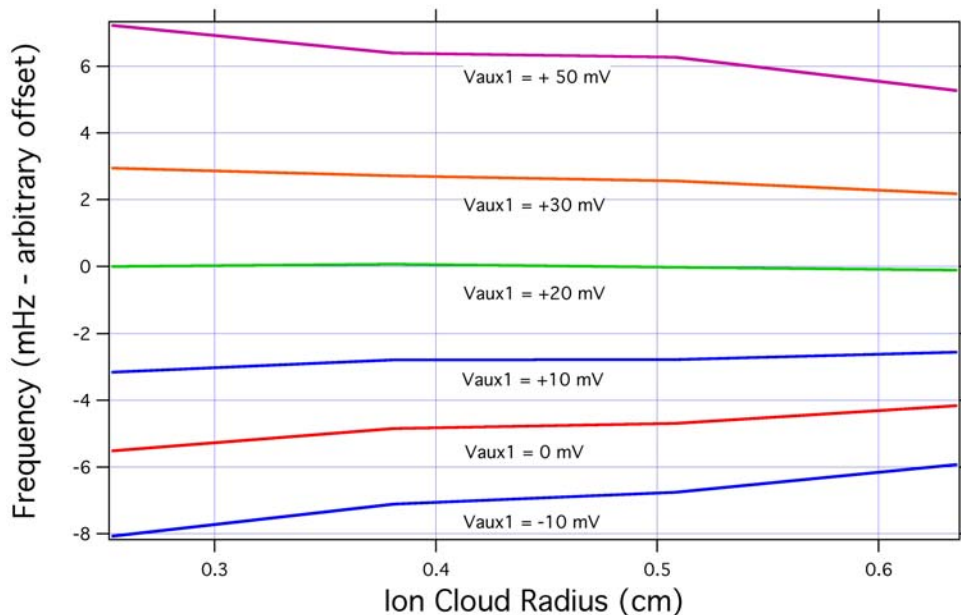

Figure 4. The average frequency shift modeled for various values of AUX1 voltage, where for each curve the axial occupation is fixed and the radial occupation is allowed to vary ("Ion Cloud Radius"). The shift is relative to a 40.5 GHz transition frequency. For clarity, an offset between each curve, as well as an overall offset, has been removed so as to better show the relative changes in slope.

The model implies that we should be able to use AUX1 to change not only the magnitude of the number-dependent shift, but its slope as well. This suggests that, in addition to simply improving field homogeniety, we may also reduce the component of the number-dependent shift that depends on trap geometry. The compensated system should yield a very small total ion number-dependent effect.

MODIFYING THE MAGNETIC FIELD ENVIRONMENT

To test this prediction, a coil was recently installed on LITS-9 at the AUX1 location. Frequency shift was measured as a function of signal size (ion number) varied by changing the load trap endcap voltage and shown in Fig. 5. Each curve in that figure represents a different AUX1 voltage, as shown.
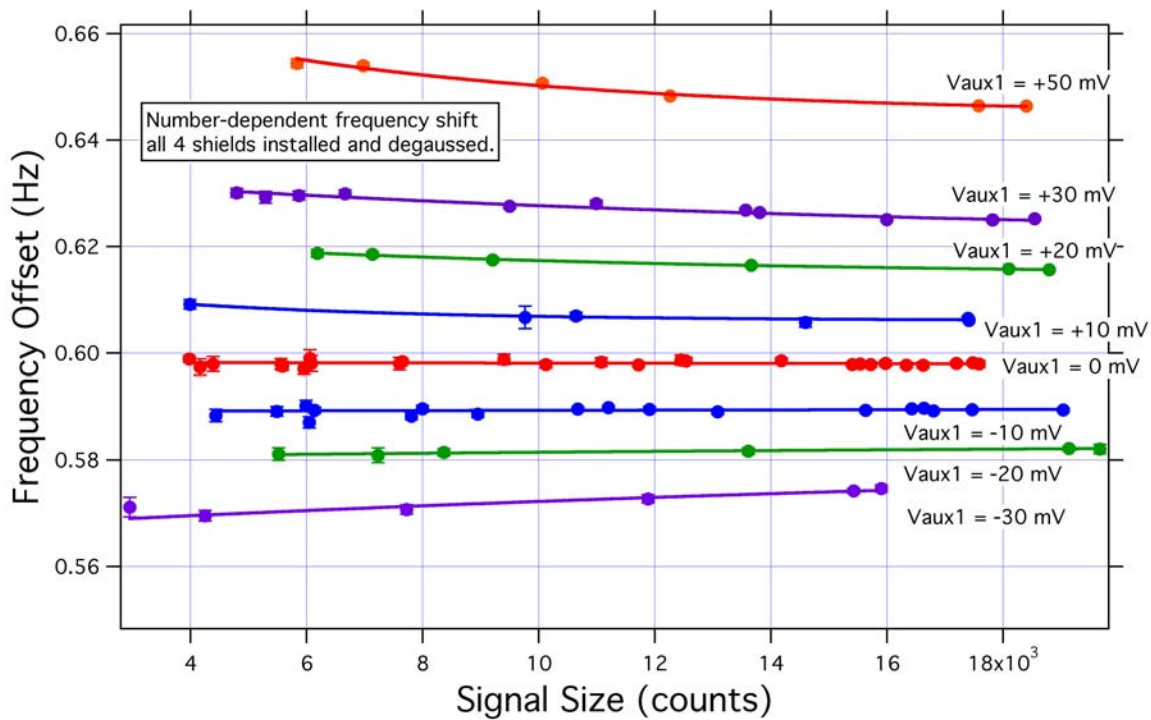

Figure 5. Measured LITS-9 frequency shifts after the magnetic shields have been degaussed. All shifts are relative to the 40.5 GHz Hg^+ clock transition frequency.

The data show good agreement with the model where the cloud expands in the radial direction, but more importantly demonstrates control over the ion-number frequency shift. The qualitative behavior is independent of shield degaussing, though degaussing introduces a different overall offset as expected. The fact that the data remain qualitatively the same before and after shield degaussing indicates that the ion-number-dependent frequency shift is not due to small field nonuniformities in the magnetic shielding, which would probably change with degaussing, but rather due to the overall geometry of the magnetic shielding and coils, which should remain constant with time up to an overall offset. As predicted by the model, the AUX1 coil allows

control not only of the offset, but also the slope of the frequency shift vs. ion number curve, thereby making it possible to cancel the two effects and greatly reduce the ion-number dependence.

OPTIMAL COIL SETTING FOR MINIMAL NUMBER-DEPENDENCE

Fig. 6 shows frequency residuals collected as a function of time, with the AUX1 coil set to 0 in (A) (compensation off) and its optimal value in (B) (compensation on). The absolute setting depends on several factors, including magnetic environment, degaussing history, as well as trap, C-field, and shield geometry and must be redetermined for each situation. In Fig. 6A, the ion number is reduced by 20% at 18,000 seconds by reducing the quadrupole trap DC bias and returned to its normal value at 36,000 seconds. The same ion number at the beginning and end of the data set enables drift removal. The frequency change during reduced ion number operation was -910(25) μHz or a fractional frequency shift of -2.2×10^{-14}. The frequency scales in (A) and (B) are the same for comparison. In (B), the ion number was reduced by 20% at 9,000 seconds and returned at 18,000 seconds (in both (A) and (B), the ion number change was made in the middle third of the data set).

The frequency change for the reduced ion number in (B) was +22(24) μHz: no shift with a fractional frequency error bar of $+5.9 \times 10^{-16}$ – a factor of almost 40 improvement. The ion number is typically stable over long time periods to 1%, which results in a systematic floor due to this effect of 3×10^{-17}.

It is essential to point out that cancellation schemes are only as good as they are stable. In this case, long-term data must be taken to verify that the optimal AUX1 coil setting doesn't vary with time. The largest potential contribution to variation would be a change in the magnetic environment. While this might be a concern for a portable standard, the magnetic environment in a metrology laboratory and specifically that of the Frequency and Timing Test Laboratory at JPL is stable to < 1 mG, so that the field as seen by the ions is stable to < 0.1 μG. This corresponds to a frequency stability of less than 2 μHz, which is several orders of magnitude smaller than the correction being made. In addition, the current source that drives the auxiliary coil is chosen so that the stability of the compensating field is better than the stability of the C-field. With these considerations, we anticipate that, after degaussing the magnetic shields, the coil setting should not need to be changed.

ESTIMATING THE NUMBER-DEPENDENT SECOND-ORDER DOPPLER SHIFT IN THE 12-POLE TRAP

In addition to estimating optimum cancellation, the model can also indicate the coil setting that gives the best field uniformity. Measuring the ion-number dependent shift at this setting provides an unmasked estimate of the actual ion-number-dependent second-order Doppler shift alone with no magnetic contribution. Fig. 7 shows the second-order Doppler shift using data taken in this way.
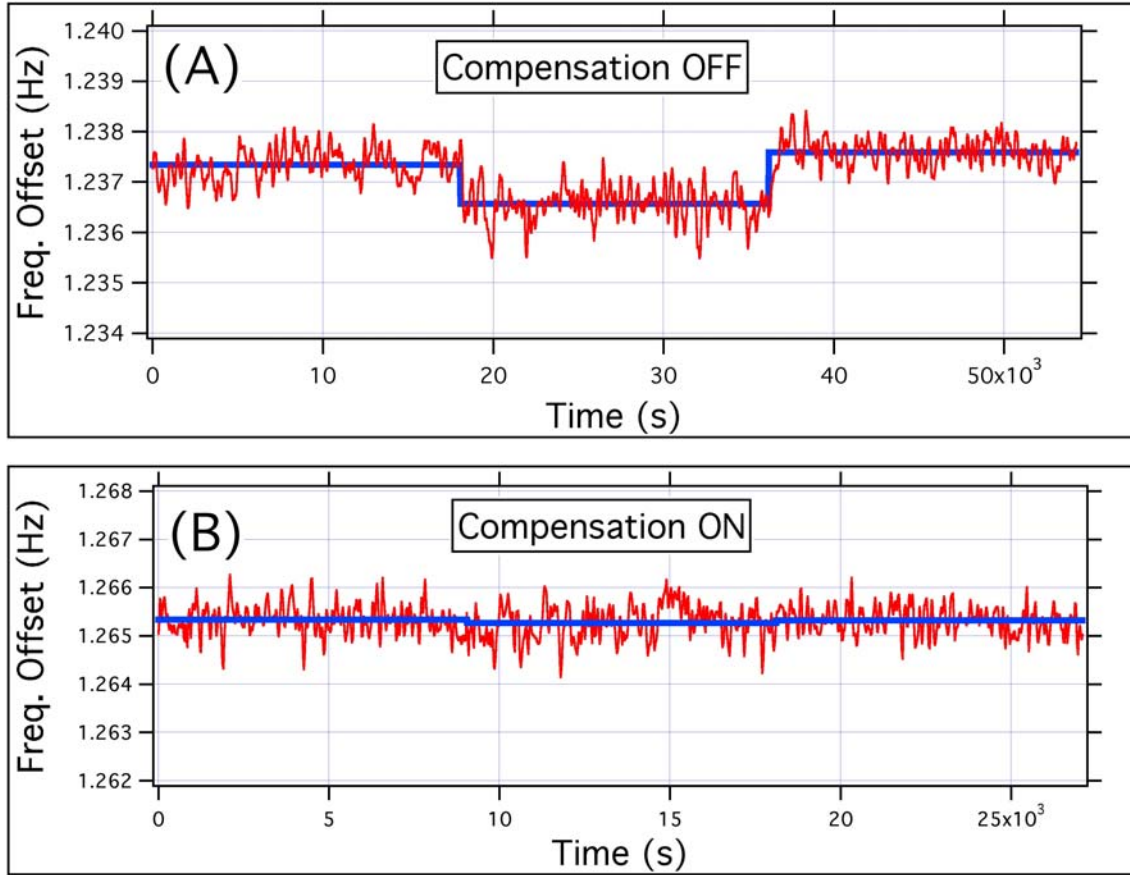
Figure 6. Frequency shift vs. ion number. In (A), frequency residuals were collected with the AUX1 coil current set to 0 (compensation off). The trapped ion number was reduced by 20% at 18,000 seconds and returned to its nominal value at 36,000 seconds. The blue line is a straight line fit to each of the three data segments. In (B), the same data are collected with the AUX1 coil current set to its optimal value (compensation on). In this case, fewer data were taken and the 20% decrease occurred at 9,000 seconds, with the return to normal ion number occurring at 18,000 seconds. The blue line here is the same fit as in (A).

As expected, the data show the dramatic reduction in this effect between the quadrupole LITS and the multi-pole LITS [4]. The pure second-order Doppler shift in the multi-pole LITS is -2 mHz (-5×10^{-14} fractional frequency) from an empty to a full trap. For comparison, the uncompensated multi-pole LITS shift is +3 mHz and the compensated multi-pole data change by -0.2 mHz.

NEON BUFFER GAS: REDUCING THE PRESSURE SHIFT

An inert background buffer gas is used to cool trapped ions. Previously, helium was chosen as the buffer gas for the LITS and fluctuations in the buffer gas pressure give the next largest systematic sensitivity after the second-order Doppler shift (see **[18]** for a list of all known LITS systematic sensitivities and **[14]** for a list of other background gas shifts – these are expected to be smaller than that of the buffer gas). Several other candidates for buffer gasses exist and it has been shown that, of these, neon has one of the smallest shifts **[13,14]**. At 8.9×10^{-9}/torr fractional frequency shift, it is approximately 3x smaller than the helium pressure shift. In addition, because of its larger mass, neon also cools mercury ions more efficiently, enabling operation at a lower buffer gas pressure. The neon buffer gas system now in use in LITS-9 employs a capillary leak instead of the heated quartz leak previously used for helium, which further improves
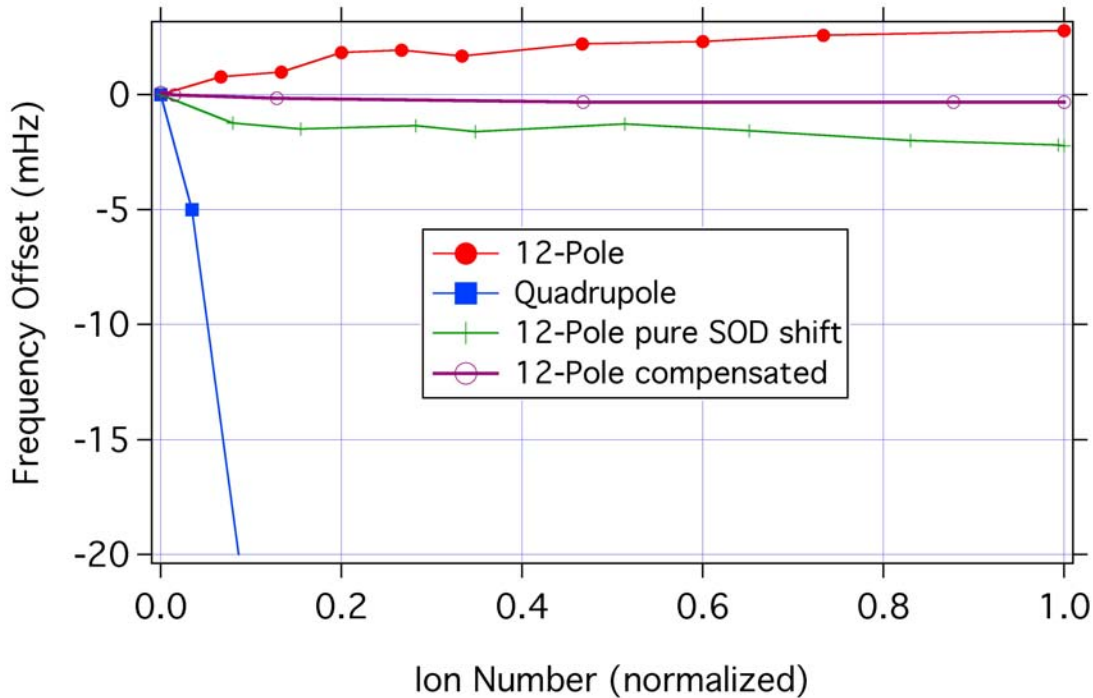

Figure 7. The total ion-number-dependent shift for the quadrupole LITS (blue squares), the uncompensated multi-pole LITS (filled red circles), the multi-pole LITS operating with AUX1 set to produce optimal cancellation of the number-dependent effect (open purple circles), and the multi-pole LITS operating with AUX1 set to produce the most uniform field, thereby showing an estimate of the pure number-dependent second-order Doppler shift (green crosses). The total fractional frequency shift for an empty to a full trap is about -3×10^{-12} for the quadrupole LITS, $+7 \times 10^{-14}$ for the uncompensated multi-pole LITS, -5×10^{-14} for the estimated pure second-order Doppler shift in the multi-pole LITS, and $< 5 \times 10^{-15}$ for the compensated multi-pole LITS.

pressure stability. The helium buffer gas system limited clock stability at about 2×10^{-16}. With neon, the smaller sensitivity, taken together with the lower neon pressure, results in about a

factor of 6x lower systematic floor due to the pressure shift or < 4x 10^{-17}. With this change, the primary multi-pole LITS sensitivities have been reduced to < $4x10^{-17}$, resulting in an expected combined systematic floor of < $5x10^{-17}$ for LITS-9.

LAMP DUTY CYCLE CONTROL: IMPROVED SHORT-TERM STABILITY

In addition to multi-pole LITS long-term stability enhancements, it is also desirable to improve the short-term stability where possible in order to average down to the systematic floor as fast as possible. The best short-term performance demonstrated in a LITS is $2x10^{-14}/\tau^{1/2}$ [1,2]. However, this was measured in a older quadrupole LITS that did not have the long-term stability benefits of the multi-pole LITS. Previously, the best short-term performance in the multi-pole LITS was about $7x10^{-14}/\tau^{1/2}$ [16]. The short-term performance of the standard is given by:

$$\sigma_y(\tau) \propto \frac{T_c^{1/2}}{f_0 T_r SNR \tau^{1/2}},$$
(2)

where T_c is the time to execute one complete cycle of the clock, f_0 is the clock frequency, T_r is the interrogation time, *SNR* is the signal-to-noise ratio of the clock signal, and τ is the averaging time (overall constants of proportionality have been left out). Beyond the simple improvement in *SNR*, a longer interrogation time will result in better stability at a given averaging time (the longer interrogation time leads to a narrower clock resonance and a larger atomic line "Q").

Trapped ion standards, with their long confinement and coherence times, are generally ideal systems for using increased interrogation times. However, the LITS uses a discharge lamp for both state selection and detection. For most discharge lamps, there is an optimal operating temperature that will produce the best *SNR* (for example, see [9]). Since the lamp is generally switched between a bright (ion loading, state selection, and state detection) and a dim (microwave interrogation) state it will reach an equilibrium temperature determined by the microwave interrogation time, thereby resulting in a T_r that optimizes SNR. Bi-modal operation of the lamp has historically been used to minimize the light shift during microwave interrogation. However, in the multi-pole LITS, ions are spatially separated from the region illuminated by the lamp. Light leakage from the loading region to the interrogation region is suppressed by a factor of ~10^4 or more, which is more than the reduction in light between the bright and dim states of the lamp. So, in the multi-pole LITS, it is acceptable to have the lamp on during microwave interrogation.

Every discharge lamp has slightly different characteristics, but as an example, the lamp currently being used in the multi-pole LITS-9 at JPL achieves optimal output to pump and detect $^{199}Hg^+$ when its bright/dim duty cycle is about 0.3. The loading, state preparation, and detection take about 4 s. Therefore, this lamp will produce optimal output if the time to shuttle ions to and from the interrogation region (about 1 s) together with the interrogation time is 9.3 s. Different interrogation times dictate a different duty cycle and equilibrium lamp temperature. Small increases in interrogation time can be achieved by externally heating the lamp to give the same equilibrium temperature as in the shorter interrogation time. In fact, this is currently

accomplished by heating the lamp enclosure allowing the interrogation time to be increased to 15 s. The temperature is controlled by a feedback loop to further improve the stability of lamp output. Now, taking advantage of the large light attenuation factor between the two trapping regions, we have the ability to increase the total interrogation time by integral multiples of the optimal lamp cycle time without changing the effective lamp output. Fig. 8 illustrates the approach.

Using this method of lamp operation, LITS-9 has been operated with a total interrogation time of 30.5 s (the lamp would not be able to support such a low duty cycle if it weren't switched to the bright state in the middle of this interrogation) without loss of SNR. This corresponds to a short-term stability of $6.1 \times 10^{-14}/\tau^{1/2}$, a record for the multi-pole LITS (see Fig. 9). It is notable that this stability is achieved without any impact on long-term systematic effects and that it is obtained using only one of the normally two detection arms. A second arm exists and, if added in with the same SNR, should yield a short-term stability of about $4 \times 10^{-14}/\tau^{1/2}$. Another advantage of long interrogation times is a reduction in sensitivity to aliasing effects [23]. Using a maser LO and shorter cycle times of between 6 and 9 seconds, down-converted noise due to aliasing limited the LITS short-term stability at about $7 \times 10^{-14}/\tau^{1/2}$ (a quadrupole LITS short-term stability of $2 \times 10^{-14}/\tau^{1/2}$ was demonstrated using a Cryogenic Sapphire Oscillator LO [2]). For the long interrogation times described here, aliasing effects should be less than $3 \times 10^{-14}/\tau^{1/2}$ and, therefore, should not limit short-term performance.

Even longer interrogation times are possible, largely limited by the coherence time of ions in the trap. Fig. 10 shows a frequency spectrum of the LITS clock transition using a 65 s interrogation time. The resulting atomic line Q (frequency divided by the full-width-at-half-maximum frequency) of 5×10^{12} is the highest ever achieved in a room temperature microwave frequency standard and within a factor of 2 of the record line Q for the microwave clock transitions measured in laser-cooled Hg^+ [17].

Fig. 11 shows an Allan deviation of frequency residuals between LITS-9 and JPL maser P26 that directly demonstrates the LITS-9 short-term performance improvement. LITS-9 uses a maser LO and, in these data, the cycle time was 26.5 s, so from 1 to 26.5 s the data show the difference between the two masers. At 26.5 seconds, the LITS-9 control loop begins to take over. At about 10,000 seconds, the Allan deviation has a combined value of 7.5×10^{-16}, to which the maser is contributing 5×10^{-16} (determined by a separate measurement). Therefore, at 10,000 seconds, the LITS-9 stability is also about 5×10^{-16} and (assuming a white noise process) has a slope of $5 \times 10^{-14}/\tau^{1/2}$. After 10,000 seconds, the maser drift becomes apparent in the measurement.

Of course it isn't possible to take advantage of long interrogation times without a local oscillator (LO) that can match the resultant stability for times at least as long as the interrogation time. For field operation, the LITS is typically configured with a quartz LO and shorter interrogation times of less than 5 s are required to avoid degradation in stability. However, the multi-pole LITS-9 is currently being configured as a laboratory reference and timekeeping standard and can use a hydrogen maser receiver as its LO. The maser receiver has stability as good or better than LITS-9 for averaging times between 10 and 1000 seconds, thereby allowing closure of the loop anywhere in this range.
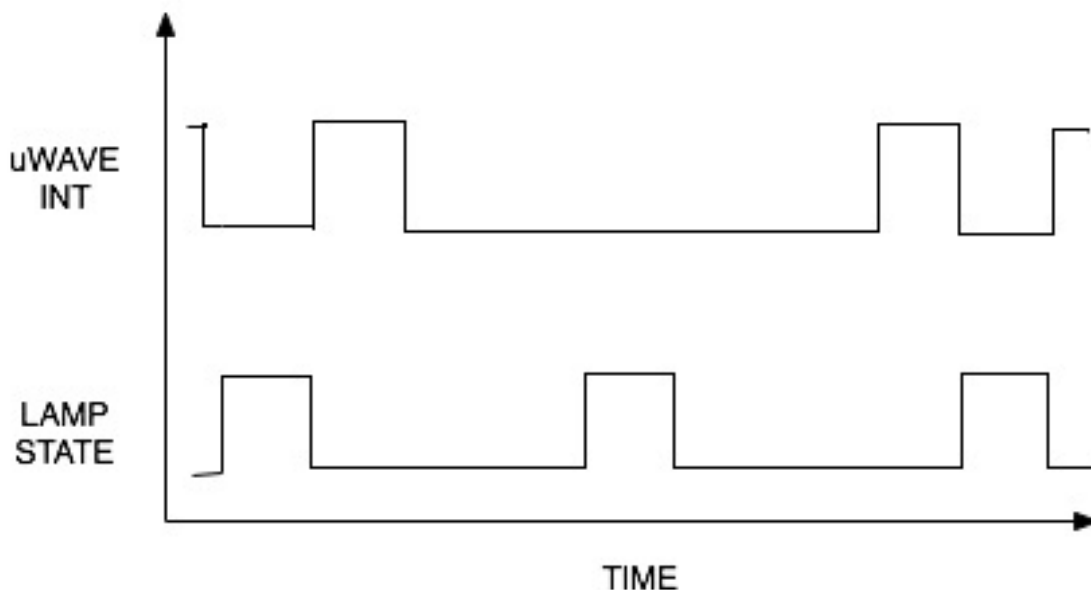
Figure 8. A timing chart showing the states of microwave interrogation and the discharge lamp as a function of time (not to scale). In this example, two-pulse Ramsey interrogation is used so that the total interrogation time consists a long "free-precession" time in between microwave pulses when the microwave field is turned off. The lamp is shown operating at an optimal duty cycle that includes a bright state during microwave interrogation.

Of course it isn't possible to take advantage of long interrogation times without a local oscillator (LO) that can match the resultant stability for times at least as long as the interrogation time. For field operation, the LITS is typically configured with a quartz LO and shorter interrogation times of less than 5 s are required to avoid degradation in stability. However, the multi-pole LITS-9 is currently being configured as a laboratory reference and timekeeping standard and can use a hydrogen maser receiver as its LO. The maser receiver has stability as good or better than LITS-9 for averaging times between 10 and 1000 seconds, thereby allowing closure of the loop anywhere in this range.

LONG-TERM COMPARISONS

Previously, LITS-8 drift relative to UTC (USNO) was measured at less than 2×10^{-16}/day **[5]**. With the compensated LITS-9, we expect this performance to be at least 10x better. However, detecting a drift of 1×10^{-17}/day is difficult. To demonstrate the new immunity to systematic effects, a comparison must be made to a clock with similar capability. In addition, given the short-term stability of the LITS, such a comparison would need to be carried out for a month or longer to allow the clock noise to average down to a value that would reveal the stability "floor." Candidate comparison references could include a second multi-pole LITS, laser-cooled atomic fountain clocks (though these generally don't operate for more than a few weeks without intervention), and ensembles of clocks such as UTC (USNO) and UTC (NIST).
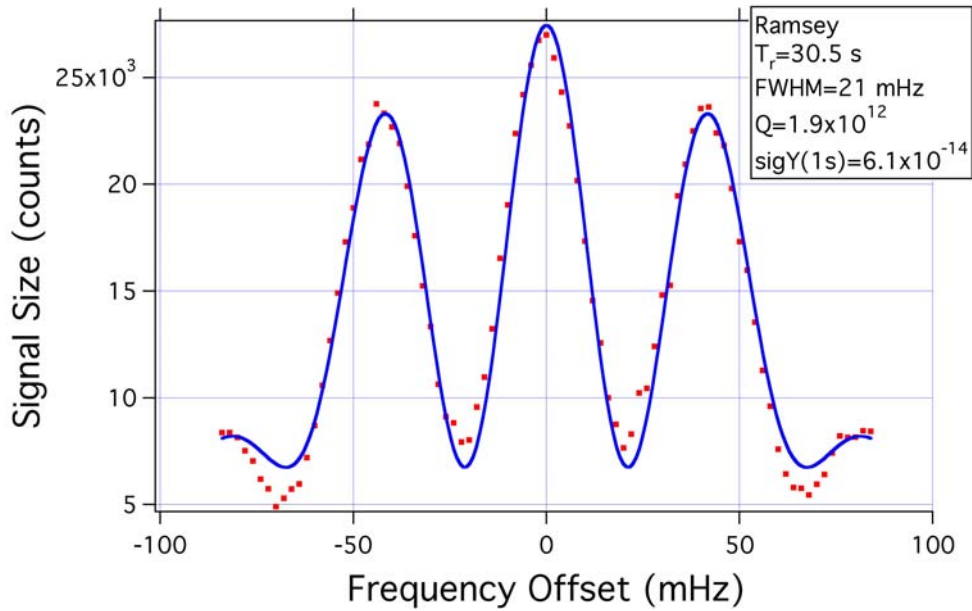
Figure 9. A frequency spectrum of the LITS clock transition using Ramsey interrogation with the interrogation time set to 30.5 s. The lamp is switched to its bright state once during interrogation. The central fringe has a FWHM of 21 mHz. The estimated short-term stability is $6.1 \times 10^{-14}/\tau^{1/2}$. The red dots are the actual data points and the blue line is a fit to a Ramsey line shape.
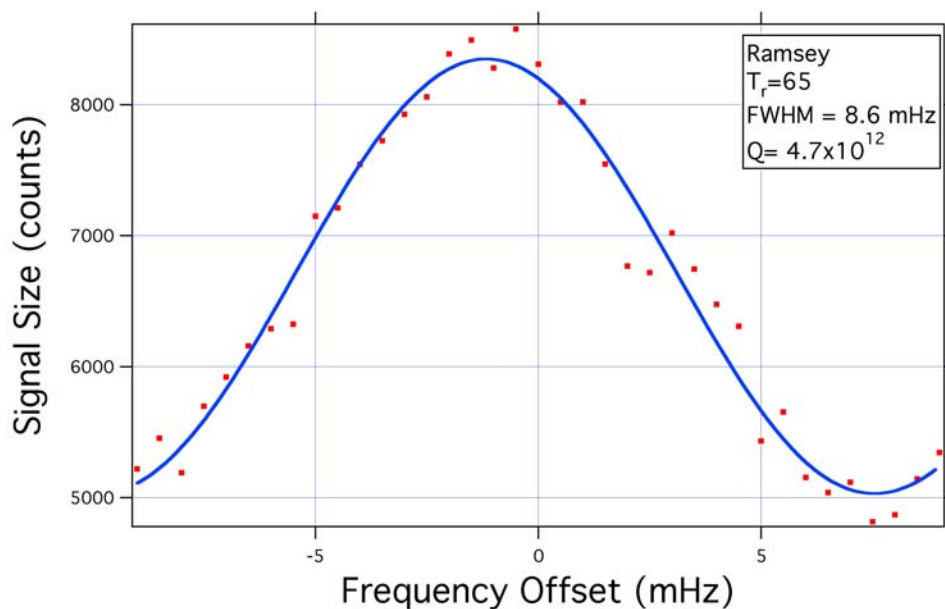

Figure 10. A frequency spectrum of the LITS clock transition using the longest interrogation time of 65 seconds using lamp switching during interrogation. The red dots are the data and the blue line is a fit to a Ramsey line shape.
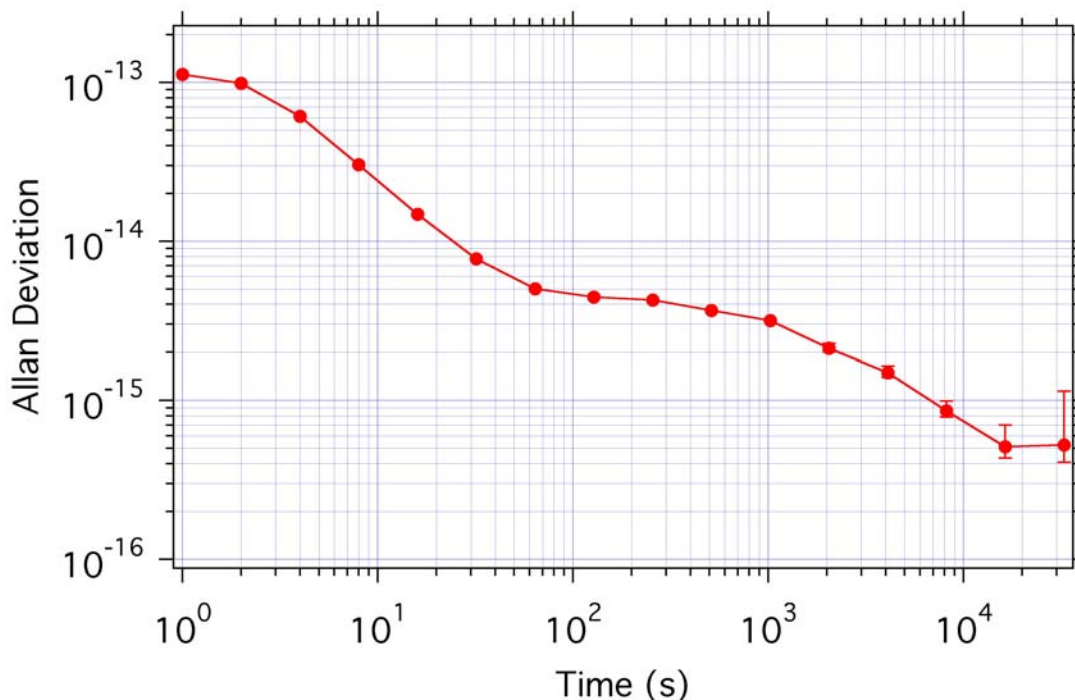
Figure 11. Allan deviation of frequency residuals between LITS-9 and JPL maser SAO-26, showing improved short-term stability. The stability is maser-limited for times greater than 10^4 seconds.

LITS-9 VS. LASER-COOLED FOUNTAINS

Laser-cooled atomic fountain clocks are currently used as primary standards, and none of these is limited by a systematic floor or drift on time scales of up to millions of seconds. While fountain clocks do not operate unattended as long as the LITS, multi-week comparisons between LITS-9 and a fountain would be very useful. We are currently in the process of co-locating JPL's laser-cooled cesium fountain [19] with LITS-9. This will allow us to make *in-situ* comparisons between the two clocks using the JPL Frequency Standard Stability Analyzer (FSSA). The noise floor of the FSSA is well below that of either clock and so will not limit the measurement on any time scale of interest [20].

COMPARISONS USING GPS CARRIER PHASE TIME TRANSFER

Until JPL's fountain clock becomes operational in its new location, it is possible to compare LITS-9 remotely to other standards using GPS Carrier Phase Time Transfer (GPSCPTT). By making LITS-9 the reference for the geodetic timing receiver (an Ashtech Z12t) whose designation is JPLT, we can compare LITS-9 to any other standard that is used as a reference for another timing receiver. Many International GNSS (Global Navigation Satellite Systems) Service (IGS) stations use a single hydrogen maser as their frequency references; however, in the case of NIST and USNO, the reference is effectively an ensemble of masers carefully steered to UTC and, thereby, to the primary standards. These ensembles should have stability that is better than any component clock, making comparisons to LITS-9 particularly interesting.

GPSCPTT data are processed using the GIPSY analysis code. Precise Point Positioning along with JPL's precise satellite orbits are used in the analysis. The comparison described here is from MJD 54015 (7 October 2006) through MJD 54071 (2 December 2006) – the first 2 months of an ongoing measurement. LITS-9 is compared to UTC (USNO) via the USNO receiver known as USN3. The reference for USN3 consists of an auxiliary offset generator, itself referenced to a hydrogen maser that is gently steered to UTC. During the entire time of this comparison, LITS-9 was operated continuously with no intervention and all data presented are from one continuous run.

GIPSY analysis produces raw phase residuals. Day-boundary discontinuities, common to GPSCPTT (for example see **[21]**), are removed by equating the phase after the day boundary to that before. Occasionally (about once or twice per month), discontinuities are found at non-day-boundaries. These are removed in the same way after verifying by local maser comparisons that LITS-9 is not the cause. It is not uncommon for the timing receiver to produce these jumps in the data **[22]** and we assume it is the source. Once discontinuities are removed, a straight line is removed from the data by matching the starting and ending points in phase. This slope in phase corresponds to the frequency offset that the LITS operates at by virtue of its C-field value. Finally, frequency residuals are calculated from the processed phase data. No drift is removed from the frequency data.

Fig. 12 shows the processed phase residuals between LITS-9 and UTC (USNO). The day-boundary discontinuities corrected in these data had zero mean, were Gaussian distributed, and had a RMS of 530 ps. During this 8-week period, LITS-9 differed from UTC (USNO) by less than ±1 ns. Fig. 13 shows the derived frequency residuals for this run. A naïve fit to a straight line gives a drift of $0(3) \times 10^{-17}$/day; that is, no detectable drift within the error bar over the 2-month period.

An Allan deviation of the frequency data is shown in Fig. 14. The behavior of the Allan deviation is typical of this form of time transfer **[21]** over long baselines: the frequency averages down as $1/\tau^p$ where $\frac{1}{2} < p < 1$ until it reaches what appears to be a floor at about 1.5×10^{-15}. Also shown in this graph are recent LITS-9 short-term ($< 10^6$ seconds) performance against a local maser and a short-term comparison between LITS-9 and LITS-8 before the latter was delivered to USNO in 2002 (this was also before the enhancements described in this paper were applied to LITS-9). A factor of $\sqrt{2}$ is removed from the LITS-9 minus LITS-8 data to reveal the underlying behavior of each individual standard. While not conclusive, the data measured locally and shown in Fig. 14 are not consistent with the 10^{-15} floor as measured by GPS, suggesting that the floor is not due to LITS-9. Near 10^6 seconds, the Allan deviation of the GPS data averages down further. While there are not enough data for the last point to be statistically significant, it is suggestive of further improvement. Perhaps just as important, these measurements are beginning to probe the capabilities of GPS time transfer for averaging times longer than 10^6 seconds without clock limitations.
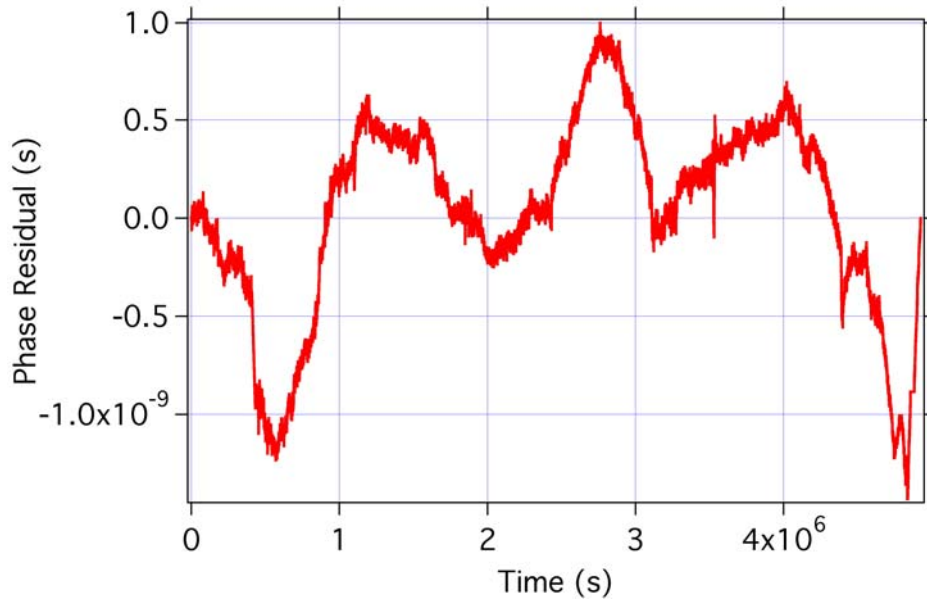
Figure 12. Phase residuals between JPLT (LITS-9 reference) and USN3 (USNO Master Clock reference) using GPSCPTT over the 2-month period from MJD 54015 to MJD 54071.
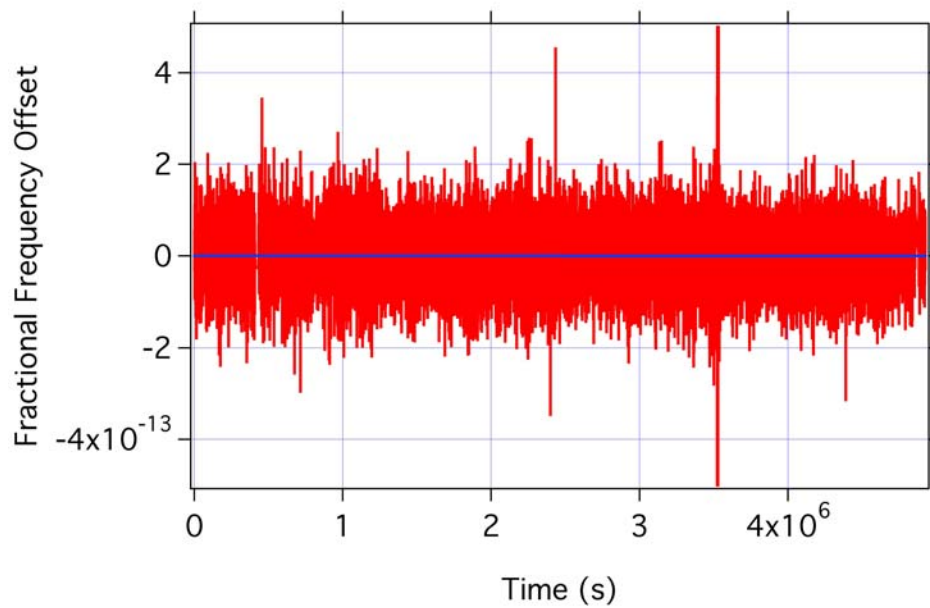

Figure 13. Fractional frequency offsets between JPLT and USN3 derived from the phase data shown in the previous figure. The blue line is a least-squares fit to the data with a straight line and gives a slope of $0(3) \times 10^{-17}$/day.
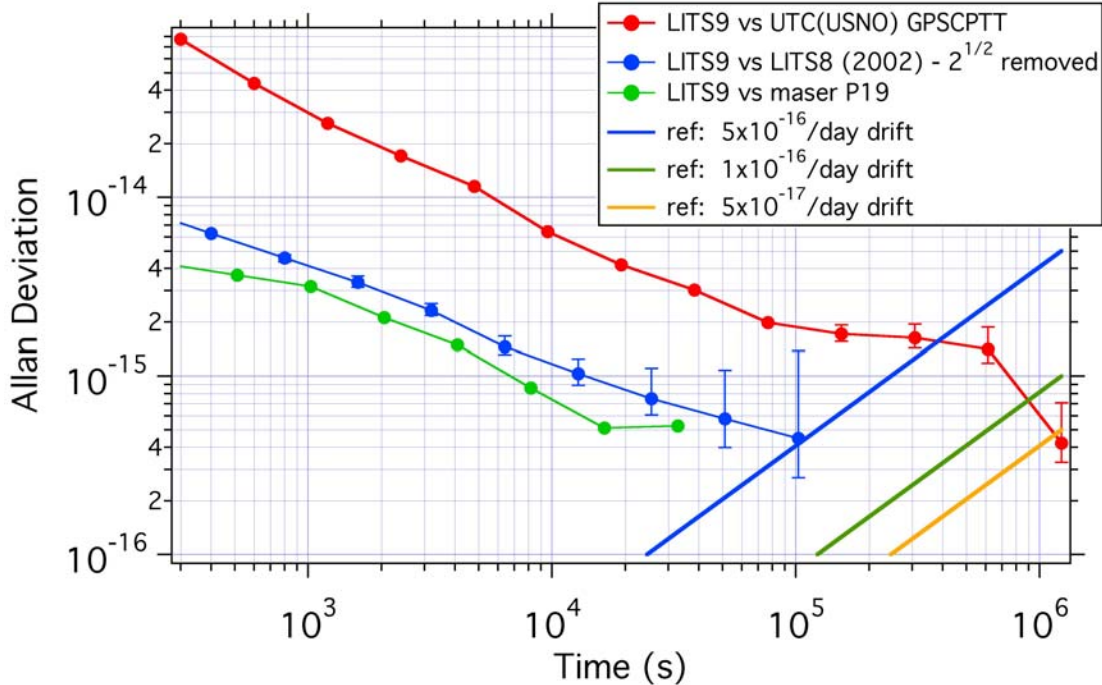
Figure 14. Allan deviation of frequency offsets shown in the previous figure. The red line is the GPS comparison data. The blue data line with solid circles is a 2002 comparison between LITS-8 and LITS-9 (before LITS-9 was upgraded) with a factor of $\sqrt{2}$ removed. The green data line with solid circles is a recent short-term comparison between LITS-9 and a local maser taken concurrent with the GPS comparison. The straight lines are various drift rates as indicated for reference. All error bars shown are 68% confidence intervals.

CONCLUSIONS

In this paper, we have verified that the source of the "anomalous" second-order Doppler shift in the multi-pole LITS is magnetic inhomogeneity, and have implemented an auxiliary coil that allows compensation of this effect to less than 3×10^{-17}. We have implemented a capillary leak neon buffer gas system that reduces sensitivity to pressure fluctuations to less than 4×10^{-17}. With these largest systematic effects reduced to these levels, the overall systematic floor of the clock is expected to be below 5×10^{-17}. Work is underway to measure the long-term stability of LITS-9 against the JPL cesium fountain atomic clock. Initial comparisons between LITS-9 and UTC (USNO) over a 2-month period show deviations of less than ±1 ns and no frequency drift with an error bar of 3×10^{-17}/day. This measurement is ongoing and we hope to present even longer data sets in the future. In addition, we have developed a new discharge lamp operating mode that has enabled improvement of the short-term stability for the multi-pole LITS to $5 \times 10^{-14}/\tau^{1/2}$. Using this mode of lamp operation, we have also achieved an atomic line Q of 5×10^{12} in the Hg^+ microwave clock transition that is the best ever observed in a room temperature microwave standard and within a factor of 2 of the best ever achieved for any microwave transition.

ACKNOWLEDGMENTS

REFERENCES

[1] R. L. Tjoelker, C. Bricker, W. Diener, R. L. Hamell, A. Kirk, P. Kuhnle, L. Maleki, J. D. Prestage, D. Santiago, D. Seidel, D. A. Stowers, R. L. Sydnor, and T. Tucker, 1996, *"A Mercury Ion Frequency Standard Engineering Prototype for the NASA Deep Space Network,"* in Proceedings of the 1996 IEEE International Frequency Control Symposium, 5-7 June 1996, Honolulu, Hawaii, USA (IEEE 96CH35935), pp. 1073-1081.

[2] G. J. Dick, R. T. Wang, and R. L. Tjoelker,1998, *"Cryo-Cooled Sapphire Oscillator with Ultra-High Stability,"* in Proceedings of the 1998 IEEE International Frequency Control Symposium, 27-29 May 1998, Pasadena, California, USA (IEEE 98CH36165), pp. 528-533.

[3] R. L. Tjoelker, J. D. Prestage, and L. Maleki, 1996, *"Record Frequency Stability with Mercury in a Linear Ion Trap,"* in Proceedings of the 5th Symposium on Frequency Standards and Metrology, 15-19 October 1995, Woods Hole, Massachusetts, USA (World Scientific, Singapore), pp. 33-38.

[4] J. D. Prestage, R. L. Tjoelker, and L. Maleki, 1999, *"Higher Pole Linear Traps for Atomic Clock Applications,"* in Proceedings of the 1999 Joint Meeting of the European Frequency and Time Forum (EFTF) and the IEEE International Frequency Control Symposium, 13-16 April 1999, Besançon, France (IEEE 99CH36313), pp. 121-124.

[5] R. L.Tjoelker, J. D. Prestage, P. A. Koppang, and T. B. Swanson, 2003, *"Stability Measurements of a JPL Multi-pole Mercury Trapped Ion Frequency Standard at the USNO,"* in Proceedings of the 2003 Joint IEEE International Frequency Control Symposium & PDA Exhibition Jointly with the 17th European Frequency and Time Forum (EFTF), 5-8 May 2003, Tampa, Florida, USA (IEEE 03CH37409C), pp. 1066-1072.

[6] R. L. Tjoelker, J. D. Prestage, and L. Maleki, 2000, *"Improved Timekeeping Using Advanced Trapped-Ion Clocks,"* in Proceedings of the 31st Annual Precise Time and Time Interval (PTTI) Systems and Applications Meeting, 7-9 December 1999, Long Beach, California, USA (U.S. Naval Observatory, Washington, D.C.), pp. 597-604.

[7] E. A. Burt, J. D. Prestage, and R.L. Tjoelker, 2002, *"Probing Magnetic Field Effects in 12-Pole Linear Ion Trap Frequency Standards,"* in Proceedings of the 2002 IEEE International Frequency Control Symposium & PDA Exhibition, 29-31 May 2002, New Orleans, Louisiana, USA (IEEE 02CH37234), pp. 463-468.

[8] J. D. Prestage, R. L. Tjoelker, and L. Maleki, 2000, *"Mercury-Ion Clock Based on Linear Multi-pole Ion Trap,"* in Proceedings of the 2000 IEEE/EIA International Frequency Control Symposium & Exhibition, 7-9 June 2000, Kansas City, Missouri, USA (IEEE 00CH37052), pp. 706-710.

[9] R. L. Tjoelker, E. Burt, S. Chung, R. Glaser, R. Hamell, L. Lim, L. Maleki, J. D. Prestage, N. Raouf, T. Radey, C. Sepulveda, G. Sprague, B. Tucker, and B. Young, 2002, *"Mercury Trapped-Ion Frequency Standard for the Global Positioning System,"* in Proceedings of the 33rd Annual Precise Time and Time Interval (PTTI) Systems and Applications Meeting, 27-29 November 2001, Long Beach, California, USA (U.S. Naval Observatory, Washington, D.C.), pp. 45-54.

[10] R. L. Tjoelker, E. Burt, S. Chung, R. Glaser, R. Hamell, L. Maleki, J. D. Prestage, N. Raouf, T. Radey, G. Sprague, B. Tucker, and B. Young, 2002, *"Mercury Trapped Ion Frequency Standard for Space Applications,"* in Proceedings of the 6th Symposium on Frequency Standards and Metrology, 9-14 September 2001, Fife, Scotland (World Scientific, Singapore), pp.609-614.

[11] J. D. Prestage, S. Chung, T. Le, M. Beach, L. Maleki, and R. L. Tjoelker, 2004, *"One-Liter Ion Clock: New Capability for Spaceflight Applications,"* in Proceedings of the 35th Annual Precise Time and Time Interval (PTTI) Systems and Applications Meeting, 2-4 December 2003, San Diego, California, USA (U.S. Naval Observatory, Washington, D.C.), pp. 427-433.

[12] J. D. Prestage, S. Chung, T. Le, L. Lim, and L. Maleki, 2005, *"Liter Sized Ion Clock with 10-15 Stability,"* in Proceedings of the 2005 Joint IEEE International Frequency Control Symposium and Precise Time and Time Interval (PTTI) Systems and Applications Meeting, 2005, Vancouver, Canada (IEEE 05CH37664C), pp. 472-476. See also J. D. Prestage, S. Chung, L. Lim, and T. Le, 2007, *"Miniaturized Mercury Ion Clock for Ultra-stable Deep Space Applications"* in Proceedings of the 38th Annual Precise Time and Time Interval (PTTI) Systems and Applications Meeting, 5-7 December 2006, Reston, Virginia, USA (U.S. Naval Observatory, Washington, D.C.), pp. 95-104.

[13] R. L. Tjoelker, S. Chung, W. Diener, A. Kirk, L. Maleki, J. D. Prestage, and B. Young, 2000, *"Nitrogen Buffer Gas Experiments in Mercury Trapped Ion Frequency Standards,"* in Proceedings of the 2000 IEEE/EIA International Frequency Control Symposium & Exhibition, 7-9 June 2000, Kansas City, Missouri, USA (IEEE 00CH37052), pp. 668-671.

[14] S. K. Chung, J. D. Prestage, R. L. Tjoelker, and L. Maleki, 2004, *"Buffer Gas Experiments in Mercury (Hg+) Ion Clock,"* in Proceedings of the 2004 IEEE Frequency Control Symposium and Exposition, 23-27 August 2004, Montreal, Canada (IEEE), pp. 130-133.

[15] W. M. Itano, L. L. Lewis, and D. J. Wineland, 1982 *"Shift of 2S1/2 hyperfine splittings due to blackbody radiation,"* **Physical Review, A25,** 1233-1235.

[16] J. D. Prestage, R. L. Tjoelker, and L. Maleki, 2001, *"Recent Developments in Microwave Ion Clocks,"* **Topics in Applied Physics, 79,** 195-211.

[17] D. J. Berkeland, J. D. Miller, J. C. Bergquist, W. M. Itano, and D. J. Wineland, 1998, *"Laser-Cooled Mercury Ion Frequency Standard,"* **Physical Review Letters, 80**, 2089-2092.

[18] E. A. Burt and R. L. Tjoelker, 2005, *"Characterization and Reduction of Number Dependent Sensitivity in Multi-pole Linear Ion Trap Standards,"* in Proceedings of the 2005 Joint IEEE International Frequency Control Symposium and Precise Time and Time Interval (PTTI) Systems and Applications Meeting, 2005, Vancouver, Canada (IEEE 05CH37664C), pp. 466-471.

[19] D. G. Enzer and W. M. Klipstein, 2004, *"Performance of the PARCS Testbed Cesium Fountain Frequency Standard,"* in Proceedings of the 2004 IEEE Frequency Control Symposium and Exposition, 23-27 August 2004, Montreal, Canada (IEEE), pp. 775-779.

[20] C. A. Greenhall, A. Kirk, and R. L. Tjoelker, 2007, *"A Multi-Channel Stability Analyzer for Frequency Standards in the Deep Space Network,"* in Proceedings of the 38th Annual Precise Time and Time Interval (PTTI) Systems and Applications Meeting, 5-7 December 2006, Reston, Virginia, USA (U.S. Naval Observatory, Washington, D.C.), pp. 105-114.

[21] See for instance A. Bauch, *et al.,*2006, *"Comparison between frequency standards in Europe and the USA at the 10^{-15} uncertainty level,"* **Metrologia, 43**, 109-120.

[22] D. Matsakis, private communication.

[23] G. J. Dick, 1987, *"Local Oscillator Induced Instabilities in Trapped Ion Frequency Standards,"* 1988, Proceedings of the 19th Annual Precise Time and Time Interval (PTTI) Applications and Planning Meeting, 1-3 December 1987, Redondo Beach, California, USA, pp. 133-147.